Cerebrospinal fluid p-tau231 as an early indicator of emerging pathology in Alzheimer's disease

Nicholas J. Ashton (nicholas.ashton@gu.se)
University of Gothenburg
Andrea L. Benedet
University of Gothenburg
Tharick A. Pascoal
McGill University
Thomas K. Karikari
University of Gothenburg
Juan Lantero-Rodriguez
University of Gothenburg
Sulantha Mathotaarachchi
McGill University
Joseph Therriault
McGill University
Melissa Savard
McGill University
Mira Chamoun
McGill University
Erik Stoops
ADx NeuroSciences
Cindy Francois
ADx NeuroSciences
Eugeen Vanmechelen
ADx NeuroSciences
Serge Gauthier
CIUSSS
Eduardo R. Zimmer
Universidade Federal do Rio Grande do Sul (UFRGS)
Henrik Zetterberg
University of Gothenburg
Kaj Blennow
University of Gothenburg
Pedro Rosa-Neto

McGill University

Research Article

Keywords: Cerebrospinal fluid, Alzheimer's, biomarkers, amyloid PET

Posted Date: January 29th, 2021

DOI: https://doi.org/10.21203/rs.3.rs-155736/v1

Version of Record: A version of this preprint was published at EBioMedicine on February 1st, 2022. See the published version at https://doi.org/10.1016/j.ebiom.2022.103836.

Abstract

Biomarkers for early phosphorylation of tau constitute an unmet need for disease modifying intervention in early stages of Alzheimer's disease (AD). Recent advances in targeted mass spectrometry and immunoassays have revealed phosphorylation sites, in the cerebrospinal fluid (CSF), with potentially greater utility as preclinical and diagnostic biomarkers as compared to the well validated biomarker – phosphorylated tau at threonine 181 (p-tau181). Phosphorylated tau (p-tau) epitopes in cerebrospinal fluid (CSF) are highly accurate biomarkers for Alzheimer's disease (AD) neuropathology and are already increased before cognitive symptoms have manifested. However, it is unknown if these preclinical increases transpire earlier, prior to amyloid-beta (Aβ) positivity threshold, and if an ordinal sequence of p-tau epitopes occurs at this incipient phase. In this study, we measured cerebrospinal (CSF) p-tau181, p-tau217 and p-tau231 in 171 participants across the AD continuum compared to AD neuropathology as indexed by Ab ([^{18}F]AZD4694) and tau ([^{18}F]MK6240) position emission tomography. CSF P-tau217 and p-tau231 predicted Aβ and tau at the preclinical and dementia stages to a similar degree but p-tau231 attained abnormal levels first. P-tau231 was more sensitive to the earliest changes in Aβ in the medial orbitofrontal, precuneus and posterior cingulate cortices before global Aβ PET positivity had been achieved. Our findings demonstrate that CSF p-tau231 increases early in development of AD pathology and is a principal candidate for detecting incipient Aβ pathology for therapeutic trial application.

Introduction

Neurofibrillary tangles (NFTs), primarily composed of abnormal hyperphosphorylated tau, are a key pathological hallmark of Alzheimer's disease (AD) [1]. Increased concentrations of extracellular soluble phosphorylated tau (p-tau) and total tau (t-tau) constitute a reliable index of this intracellular process in mild cognitive impairment due to AD [2,3] and AD dementia [2,4]. NFTs are present many years after the deposition of extracellular amyloid-beta (Aβ) plaques but are more closely related to symptom onset and longitudinal studies have demonstrated that soluble p-tau and t-tau are increased already in preclinical disease (*e.g.*, no cognitive impairment but evidence of AD pathology) [5,6]. Specifically, CSF concentrations of t-tau and p-tau are proposed to reflect neurodegeneration and tau pathology in the form of NFTs, respectively [7]. However, these biomarkers remain at normal concentrations in other neurodegenerative disorder with substantial neurodegeneration [8-10], and also those with tau pathology [11-13]. Preclinical studies provide compelling evidence supporting early brain amyloidosis as a driver of tau hyperphosphorylation in AD [14,15]. Interestingly, evidence from AD neuronal culture models indicate that soluble Aβ oligomers (AβOs) induce tau hyperphosphorylation in multiple sites [16,17]. Indeed, the link between early cerebral Aβ deposition and CSF p-tau elevations has been further supported by the fact that CSF tau species precede tau Positron Emission Tomography (PET) abnormalities by a decade [18,19]. Thus, it is suggested that CSF p-tau biomarkers likely indicate an active process of tau secretion, and one that is correlated with cerebral Aβ deposition in early disease [20-22].

CSF p-tau, in the context of AD, is often assumed to be the residue phosphorylated at threonine 181 (p-tau181). A multitude of mid-domain and C-terminal residues have also been described to be abnormally phosphorylated in the AD clinical spectrum [11,23-26] and studies specifically assessing their comparative diagnostic performance remain limited. Recent reports have suggested that CSF p-tau217 might better discriminate AD from other neurodegenerative diseases [24,27,28] than CSF p-tau181. In addition, CSF p-tau217 correlates better with Aβ and tau PET imaging than CSF p-tau181 [24]. These findings support an emerging framework suggesting that certain CSF tau phosphorylation species to predominate across the AD continuum [24,27]. We have recently reported that CSF p-tau231 increases early in the AD continuum and, therefore, may detect preclinical AD among cognitively unimpaired (CU) individuals [29]. This is of fundamental importance for identifying individuals with subtle AD-related preclinical brain changes for therapeutic trials, as it anticipates which disease-modifying drug candidates have a better opportunity to show effectiveness if initiated before symptom onset or even before the threshold of Aβ positivity has been achieved. Indeed, a recent study in transgenic mice suggests that early removal of Aβ seeds, before Aβ deposition becomes detectable, led to a significant reduction of Aβ accumulation and downstream pathologies [30]. This emphasizes the need of a biomarker for detecting early Aβ seeds or the “pre-amyloid” phase. Therefore, it is imperative to investigate CSF p-tau epitopes associated with the earliest Ab measures in CU to determine which of these early tau phosphorylation sites better reflects emerging Ab pathology.

In order to address this knowledge gap, we investigated whether CSF p-tau epitopes (p-tau181, p-tau217 and p-tau231) are capable of identifying early Aβ pathology at the clinical, preclinical and pre-amyloid phases of AD. We also tested the performance of CSF p-tau181, p-tau217 and p-tau231 as biomarkers to predict clinical outcomes and Aβ and tau PET status. Based on our previous data [29], we hypothesized that CSF p-tau231 associates with early Ab pathology in brain regions that are affected early in the AD process. For these purposes, we performed voxel-wise analyses of the association between different CSF p-tau biomarkers and Ab and tau PET in cognitively unimpaired (CU) and impaired (CI) individuals.

Materials And Methods

Study Design

The main objective of this study was to investigate whether CSF p-tau epitopes are capable of identifying early Aβ deposition before Aβ PET positivity. We also aimed at comparing their performance to predict amyloid and tau pathologies indexed by PET in participants ranging within the AD continuum. This cross-sectional study was based on data from the Translational Biomarkers in Aging and Dementia (TRIAD) cohort, which is an observational and longitudinal biomarker-based study. TRIAD participants, mostly ranging in the AD spectrum, are followed yearly with detailed clinical and neuropsychological assessments, as well as with collection of fluid (blood, urine and CSF) and acquisition of multiple imaging biomarkers. In addition to meeting standard diagnostic criteria, AD dementia participants had

CDR between 1 and 2, subjects with mild cognitive impairment (MCI) had a CDR of 0.5 and CU subjects had a CDR of 0. MCI participants without Aβ pathology are considered as non-AD neurodegenerative disease together with participants clinically diagnosed with frontotemporal dementia (FTD; clinical diagnosis of behavioral or semantic variant of FTD, CDR score>0.5 and Aβ PET negative). This article includes 171 participants (27 young, <30 years old); 82 CU; 20 MCI; 21 AD; 21 non-AD) from which CSF and PET imaging were available on October 2019.

The TRIAD study was approved by The Research Ethics Board of the Montreal Neurological Institute as well as the Faculty of Medicine Research Ethics Office, McGill University, and all study participants provided written informed consent.

CSF Analysis

CSF samples were collected by syringe and transferred to polypropylene tubes for centrifugation at 20^{o}C, 2200*g* for 10 min. Samples were then aliquoted in 1mL polypropylene vials and permanently stored at -80^{o}C pending analyses.

All samples were analyzed for p-tau181, p-tau217 and p-tau231. P-tau181 and p-tau217 were quantified by novel single molecule array (Simoa) assay that have been previously described [28,29]. In brief, rabbit polyclonal antibody specific for p-tau217 (#44-744, Invitrogen) and mouse AT270 mouse monoclonal antibody (MN1050; Invitrogen, Waltham, MA, USA) were used as capture, conjugated to paramagnetic beads (#103207, Quanterix). The mouse monoclonal antibody Tau12 (#806502, BioLegend) raised against the N-terminal epitope 6-18aa was used for detection [31]. The assay calibrator was recombinant full-length tau-441 phosphorylated in vitro by glycogen synthase kinase 3β (#TO8-50FN, SignalChem). Calibrators and specimens were diluted with assay diluent (Tau 2.0 buffer; #101556, Quanterix). Analytical validation and assay measurement protocol for both CSF p-tau181 and CSF p-tau217 Simoa assays have been previously described [28]. Both methods demonstrated intra and inter assay variation <8%. CSF p-tau231 was quantified using a research ELISA assay using cis-conformational selective monoclonal antibody (ADx253, ADx NeuroSciences). New monoclonal mouse antibodies were generated using a 17-mer synthetic peptide, phosphorylated on hTau corresponding Thr231, spanning the tau region K_{224}KVAVVR(pT)PPKSPSSAK_{240}C as a KLH-coupled antigen. Candidate hybridomas were selected on brain extracts of AD and control brain tissue. The final cloned and purified monoclonal antibody, ADx253, was characterized on synthetic peptides spanning the region T217 till S241 for its affinity, its phospho-specificity using both phosphorylated and non-phosphorylated peptides and its preferred selectivity in which proline at position 232 was replaced by a Pip (pipecolinic acid, piperidene-2-carboxylic acid, homoproline), to simulate cis-selectivity of ADx253 [32]. A pan-tau mouse mAb (ADx205, ADx NeuroSciences) with epitope in the mid tau region was used in biotinylated form as pairing antibody in the p–tau231 ELISA assay. ADx205 was recently fine-mapped using overlapping

linear synthetic peptides and the ADx205 antibody was found to bind between R_{194} and G_{204} of tau441 or 2N4R tau sequence.

Imaging Analysis

All participants have acquired 3T T1-weighted images for coregistration purposes. In addition, a Siemens High Resolution Research Tomograph (HRRT) was used for PET imaging acquisitions. For Aβ PET, images were acquired 40–70 minutes post-injection of [^{18}F]AZD4694 and scans were reconstructed using the ordered subset expectation maximization (OSEM) algorithm on a 4-dimensional volume with 3 frames (3 x 600s) [33]. For tau PET, [^{18}F]MK6240 scans were acquired 90–110 minutes post-injection and the OSEM algorithm was also used for reconstruction on a 4D volume with 4 frames (4 x 300s) [34]. Additional pre-processing corrections were performed as described elsewhere [35]. PET images were meninges and skull stripped, linearly and non-linearly registered to the ADNI template space and then spatially smoothed to achieve a final resolution of 8 mm FWHM [36]. The inferior cerebellum and whole cerebellum gray matter were used as the reference regions for [^{18}F]MK6240 and [^{18}F]AZD4694, respectively.

Global Aβ PET used averaged SUVR of the precuneus, cingulate, inferior parietal, medial prefrontal, lateral temporal, and orbitofrontal cortices [37] and positivity was visually defined by two neurologists blinded to clinical diagnosis. An additional Aβ PET SUVR cutoff value of 1.55 was estimated as previously described [38]. Aβ PET SUVR was also converted to Centiloid units [39] as previously described [38,40]. The PET SUVR cutoff value of 1.55 corresponds to 24 Centiloids. Tau PET SUVR was globally estimated from a composite area including the transentorhinal (Braak stage I-II) and limbic (Braak III-IV) cortices [41,42]. Tau positivity was here defined as 2.5 standard deviations (SD) higher than the mean global SUVR of the young participants (cutoff = 1.03).

Statistical Analysis

All non-imaging statistical analyses were performed using the R programming language (version 3.4.3). Cross-sectional demographic and clinical data were assessed with *t* tests and χ^2 tests. Spearman rank correlation tests were applied to evaluate the association between biomarkers and correlation coefficients were compared using the R package "*Cocor*". Linear regression models also tested the association between log-transformed CSF p-tau and other biomarkers always adjusting by age and gender. Similar models were also applied to evaluate group differences and, when necessary, Tukey honestly significant difference (HSD) test was used in the post hoc analysis. Receiver operating curves (ROC) provided both the area under the curve (AUC), for AD diagnosis or biomarker positivity, and the representative best value for accuracy at an optimal cutoff value. In addition to AUC, sensitivity and specificity, paired Delong's test

(*pROC* R package) was applied to statistically compare biomarker performance. Finally, imaging and CSF cutoffs were used to evaluate concordance between biomarkers.

Voxel-wise analyses were performed using VoxelStats [43]. Voxel-based linear regression models evaluated the correlation between log transformed [44] was used to correct the resulting *t* parametric maps for multiple comparisons (one-sided). In order to compare the effect of CSF biomarkers on the PET biomarkers, the adjusted R-squared values of the models were averaged within ROIs encompassing only the voxels that were significantly associated to all CSF biomarkers simultaneously. The ROIs include precuneus, posterior cingulate, frontal orbital gyri, post central gyri and medial frontal gyri for Aβ PET, whilst for tau PET they were the average of Braak I-II, Braak III-IV and Braak V-VI staging regions.

CSF biomarkers were also plotted as a function of Aβ PET, which served as a proxy of disease progression. For that, Aβ PET values were given in Centiloid units and CSF biomarkers were first adjusted by age and sex and only then transformed in Z-score values based on the average and standard deviation of the CU population. Finally, a locally weighted polynomial regression method was employed, using the *lowess* function in R, with 0.7 smoother spam.

Results

Participants

This study included 171 participants, stratified in CU = 109 (23% Aβ PET+) and CI = 62 (66% Aβ PET+) groups (Table 1), with cross-sectional CSF (p-tau181, p-tau217, p-tau231) and PET ([^{18}F]AZD4694 and [^{18}F]MK6240). The same participants were also categorized as CU (Aβ+/-), MCI, AD and non-AD (supplementary table 1, online resource). The mean age of the population was 62.77 years, with CI participants being older than CU (CU = 59.82; CI = 67.78; $P < 0.001$) owing to a proportion of the CU being < 30 years in age (n = 27). As expected, the CI group had a lower MMSE scores and higher Aβ PET and tau PET load as compared to the CU group (Table 1). *APOE*-e4 carriers and males were also more abundant in the CI group. Older age was associated with higher levels of all CSF p-tau. There was no association between sex and p-tau biomarkers when adjusting for age and diagnosis.

Group comparisons

CSF p-tau biomarkers were highly correlated, in the whole cohort, and in diagnostic categories groups (supplementary fig. 1A–E, online resource) with the strongest association being between CSF p-tau217 and CSF p-tau231 in whole cohort ($r = 0.92$, $P < 0.001$) and in the CI group ($r = 0.93$, $P < 0.001$). Within the CU group, the strongest association was found between CSF p-tau181 and CSF p-tau231 ($r = 0.86$, $P < 0.001$).

When assessing groups as either CU or CI, all CSF p-tau biomarkers were significantly increased in Aβ+ groups as compared to Aβ- groups (Fig. 1A–C). Interestingly, CSF p-tau231 (Fig. 1A) and CSF p-tau217 (Fig. 1B) were significantly increased in CU Aβ+ as compared to CI Aβ- but this was not observed for CSF p-tau181 (Fig. 1C). CSF p-tau217 was 6-fold higher in CI Aβ+ than in CU Aβ-, which was a significantly larger increase than other p-tau biomarkers ($P_{p\text{-}tau231}$=0.002; $P_{p\text{-}tau181}$=0.01; supplementary table 2, online resource). Similarly, CSF p-tau217 demonstrated the largest fold increase between CI Aβ+ and CI Aβ- (4.7-fold, $P < 0.002$; supplementary table 2, online resource). However, this was not significantly different to other CSF p-tau biomarkers. CSF p-tau biomarkers concentrations were also visualized by specific diagnostic categories (Fig. 1D–F) and fold change (supplementary table 2, online resource). This analysis further demonstrated that CSF p-tau217 had a superior fold changes to other p-tau biomarkers ($P < 0.02$) when specifically comparing MCI Aβ+ and AD dementia with CU Aβ- (MCI Aβ+, 5.9-fold; AD, 7.1-fold) and non-AD neurodegenerative disorders (MCI Aβ+, 4.8-fold; AD, 5.8-fold).

Performance of CSF p-tau in clinically defined groups

Next, we investigated the diagnostic accuracy of CSF p-tau biomarkers in differentiating clinical categories not determined by underlying Aβ and tau PET status (supplementary table 3, online resource). In a ROC analysis, CSF p-tau181 was the best performer in distinguishing between CU and AD when Aβ and tau PET status were unknown (AUC = 0.97; 95% CI, 0.95-0.99). This significantly outperformed CSF p-tau231 but not CSF p-tau217. All biomarkers had high accuracies (AUC > 0.96) in separating AD from non-AD and no biomarker was found to be statistically greater in this comparison. A noticeable decline in performance was observed for CSF p-tau181 when distinguishing MCI from non-AD (AUC = 0.83; 95% CI, 0.67-0.99) and MCI from CU (AUC = 0.81; 95% CI, 0.66-0.96). No such changes were observed for other biomarkers demonstrating that CSF p-tau181 is not sensitive to early pathological changes but an accurate biomarker at late stage disease.

Associations between CSF p-tau biomarkers with tau PET

Tau PET was performed in all 171 participants included in this study. High concentrations of all CSF p-tau biomarkers were associated with increased retention of [^{18}F]MK6240 composite Braak stage I-IV. A similar correlation coefficient was observed between CSF p-tau231 ($r = 0.74$, $P < 0.001$, supplementary fig. 2A, online resource) and CSF p-tau217 ($r = 0.73$, $P < 0.001$, supplementary fig. 2B, online resource) with Braak stage I-IV. In contrast, significantly inferior correlations ($P_{\text{p-tau231 vs p-tau181}}$= 0.004; $P_{\text{p-tau217 vs p-tau181}}$= 0.02) were observed for CSF p-tau181 ($r = 0.66$, $P < 0.001$, supplementary fig. 2C, online resource). No significant differences were found between the CSF biomarkers when predicting tau PET positivity and all demonstrated comparable AUC values (AUC = 0.91-0.97, supplementary fig. 2D, online resource).

At the voxel level, CSF biomarkers were associated with higher [^{18}F]MK6240 uptake in the inferior, medial and lateral temporal regions (T_{all}>3.14; P_{all}<0.05, Fig. 2A), with associated areas overlapping between CSF biomarkers. No marked difference was observed between CSF p-tau231 and CSF p-tau217, whilst CSF p-tau181 indicated weaker associations narrowed to reduced regions if compared to the other biomarkers (Fig. 3A). When groups were evaluated as CI (Fig. 2B) and CU (Fig. 2C) separately, broad associations were found in the CI group (T_{all}>3.25; P_{all}<0.05, Fig. 2B), where high concentrations of CSF biomarkers were associated with high [^{18}F]MK6240 binding in the temporal lobes, cingulate regions and orbitofrontal cortices, encompassing Braak stage regions I-VI. A stronger relationship between [^{18}F]MK6240 and CSF p-tau231 and CSF p-tau217 (T>3.16; P<0.05) where found in CU participants, with significant associations confined to temporal regions corresponding to Braak stage regions I-IV (Fig. 2C).

Associations between CSF p-tau biomarkers with Aβ PET

Aβ PET was performed in all 171 participants included this study. In a similar findings to tau PET, correlation coefficients where strongest between [^{18}F]AZD4694 global retention and CSF p-tau231 (r = 0.81, P < 0.001, Fig. 3A) and CSF p-tau217 (r = 0.79, P < 0.001, Fig. 3B). Once more, correlations were inferior for CSF p-tau181 (r = 0.70, P < 0.001, Fig. 3C) which were significantly different to other p-tau biomarkers ($P_{\text{p-tau231 vs p-tau181}}$< 0.001; $P_{\text{p-tau217 vs p-tau181}}$= 0.01). CSF P-tau231 (AUC = 0.95; 95% CI, 0.92-0.98) and CSF p-tau217 (AUC = 0.95; 95% CI, 0.92-0.99) were significantly better predictors of Aβ PET status than CSF p-tau181 (both P < 0.01, Fig. 3D). No significant difference was found between CSF p-tau231 and CSF p-tau217 in the prediction of Aβ PET status. To further investigate these associations, biomarker accuracy to detect Aβ positivity was evaluated within CU and CI groups separately (supplementary fig. 3, online resource). In CU individuals, CSF p-tau231 (AUC = 0.91; 95% CI, 0.84-0.98) was significantly superior to CSF p-tau181 (P < 0.01). Conversely, in CI individuals, no CSF p-tau was found to be significantly superior, although CSF p-tau217 had numerically the highest AUC (0.99; 95% CI, 0.99-1.00).

Results of the voxel-wise analysis showed high CSF biomarker levels being associated with high [^{18}F]AZD4694 binding in frontal, precuneus, posterior cingulate and temporal cortices (T_{all}>3.14; P_{all}<0.05, Fig. 4A). Even though there was a topographical overlap of the significantly associated regions between the CSF biomarkers evaluated, a markedly stronger association was observed for CSF p-tau231 when the whole sample was analyzed (Fig. 4A). In the CI group analyses, there was no marked difference between the associations of [^{18}F]AZD4694 with CSF p-tau231 and CSF p-tau-217 (T_{all}>3.25; P_{all}<0.05; Fig. 4B). In contrast, in the CU group, there was an evident difference between CSF p-tau231 and the other biomarkers (Fig. 4C), despite that the associated regions did not differ from the results reported with the whole set of participants (T_{all}>3.16; P_{all}<0.05). As an additional comparison between biomarkers in the CU group, the average beta values from the linear models were computed at the voxel-level and then averaged within ROIs. For all the regions evaluated, CSF p-tau231 had the highest beta values as

compared to the other biomarkers globally and in all ROIs (Fig. 5A). To support these initial findings, we used Aβ PET (in Centiloids) as a proxy of AD progression and we estimated at which point the relationship between the CSF p-tau231, CSF p-tau217 and CSF p-tau181 changes in relation to the disease in the whole study population (Fig. 5C). To perform this, we used locally-weighted polynomial regression analysis in which CSF biomarker levels were transformed into Z-scores and 2 Z-scores was defined as the cut-off value for biomarker positivity. No difference between the inflection point of these biomarkers was identified. Contrarily, CSF biomarkers showed to become abnormal at different pathological stages, with CSF p-tau231 status being positive at Centiloid 37.4, followed by CSF p-tau181 at Centiloid 47.3 and CSF p-tau217 at Centiloid 50.6 (Fig. 5B).

CSF p-tau231 in emerging amyloid-beta pathology

Considering the visually marked stronger association between CSF p-tau231 and [^{18}F]AZD4694 within the CU group (Fig. 4C), as compared to the other CSF biomarkers, we further investigated how these associations would be within the subjects in the earliest possible process of Aβ accumulation. Therefore, we repeated the voxel-wise analysis only in individuals classified as CU Aβ-. Interestingly, CSF p-tau231 was the biomarker that best associated with [^{18}F]AZD4694 uptake (T_{all}>3.19; P_{all}<0.05) which was significantly superior to CSF p-tau217 and CSF p-tau181 biomarkers in this analysis (Fig. 6A). These associated areas were very focal and included the medial orbitofrontal, precuneus and posterior/isthmus cingulate cortices. In order to further support the findings suggesting that CSF p-tau231 best reflects the earliest Aβ dysmetabolism, we repeated locally-weighted polynomial regression analysis, and re-estimated at which point the relationship between the CSF p-tau231, CSF p-tau217 and CSF p-tau181 changes in relation to the disease within the CU group (Fig. 7B). Again, no significant difference was observed between the inflection point of these biomarkers however, abnormality of CSF p-tau231 were observed far earlier (Centiloid 38.3) than whilst CSF p-tau217 and CSF p-tau181 (Centiloids >50). Thus, this analysis suggests CSF p-tau231 as the biomarker with the fastest preclinical increases which is the first to present abnormal levels as Aβ accumulates in the brain of emerging AD pathology.

Discussion

The present study examined the relationship between CSF p-tau biomarkers (p-tau231, p-tau217 and p-tau181) with amyloid and tau PET in 171 individuals across the AD continuum. Specifically, we demonstrate that CSF p-tau231 and CSF p-tau217 biomarkers have a similar relationship with [^{18}F]MK6240 and [^{18}F]AZD4694, being both better predictors of PET status in comparison with CSF p-tau181. At the voxel level, however, CSF p-tau231 had a markedly stronger relationship with Aβ pathology in CU individuals. Our main finding suggests that CSF p-tau231 abnormality arises during the lag phase of Aβ protein aggregation in the brain as shown by markedly stronger focal associations of CSF p-tau231 and Aβ PET in CU individuals without positive global Aβ burden. Furthermore, we demonstrated that CSF

p-tau231 displays the largest effect size in relation to Aβ deposition, both globally and regionally, and, amongst the biomarkers tested, is the first to achieve abnormal values.

The formation of NFT by the aggregation of tau is a fundamental hallmark of AD pathogenesis. However, in what way the differential release of soluble phosphorylated tau into the CSF relates to the development of Aβ and NFT pathologies, and consequently neurodegeneration, remains to be clarified. It is also unclear whether extracellular soluble phosphorylated tau is a driver of tau propagation in AD [45,46]. Our data, like prior studies [18,28,29], shows an increase of CSF p-tau epitopes in the preclinical phase of the disease, prior to symptom onset and before substantial tau PET ligand retention. We also confirm that CSF p-tau do not increase in non-AD dementias or cognitive impairment without Aβ pathology. Thus, in relation to sporadic AD, this study adds further support to the hypothesis that CSF p-tau is closely related to Aβ-mediated tau release from neurons [19] and challenges the notion of being simply a state marker of NFT or neurodegeneration. However, while it is presumed that p-tau secretion, and subsequent increase in CSF, occurs after globally aggregated Aβ, our data shows that CSF p-tau already changes with subtle Aβ pathology and therefore occurs considerably earlier than previously anticipated. This is more apparent for CSF p-tau231, which changes with Aβ deposition in the medial orbitofrontal, precuneus and posterior cingulate cortices before Aβ PET positivity is achieved. Thus, one could propose that increases in CSF p-tau231 are related to early Aβ seeds and could act as a key biomarker for the recently described “pre-amyloid phase” of AD, which occurs before Aβ deposition threshold [30].

CSF p-tau231 has been widely reported as a biomarker to detect AD at both the MCI and dementia stages of disease [11,47-51] but often it has been concluded these changes are not different from CSF p-tau181 when directly compared [52]. Yet, most of these studies did not evaluate the unimpairment phases of the AD continuum. Previous neuropathological findings, which motivated the CSF assay development of p-tau231, highlighted that a key component of pre-tangle pathology was phosphorylation at threonine 231 [53] and that CSF p-tau231 is an important discriminant of Braak 0-I from more advanced Braak stages [54]. Tau phosphorylation at threonine 231 is one of the earliest events in the cascade of phosphorylation [55], that modulates tubulin assembly [56]. Interestingly, soluble AβOs are known to hyperphosphorylate tau at threonine 231 in primary neuronal cultures. Thus, one could suggest that increased levels of CSF p-tau231 may reflect early AβOs synaptotoxicity [16]. Therefore, now that we can monitor the *in vivo* development of Aβ and tau pathologies by PET, it is not surprising that our analysis concludes that CSF p-tau231 is an early marker of emerging AD pathology in the phase when only subtle brain amyloidosis is apparent. Although CSF p-tau231 demonstrated numerically identical AUC’s to CSF p-tau217 in the prediction of Aβ PET at CU stage of the AD continuum, only CSF p-tau231 and not CSF p-tau217 was significantly superior to CSF p-tau181. Furthermore, at the voxel-wise level, CSF p-tau231 demonstrated substantially higher associations with [^{18}F]AZD4694 retention than CSF p-tau217 in CU individuals. We further performed a voxel-wise analysis in CU participants without prominent Aβ pathology (Aβ-). This concluded focal associations of CSF p-tau231 with emerging Aβ pathology in the medial orbitofrontal, precuneus and posterior/isthmus cingulate cortices which were stronger than what was observed for CSF p-tau217. Previously, Palmqvist et al. [57] also demonstrated that Aβ fibrils begin to

accumulate early in core regions of default mode network (DMN), namely precuneus, posterior cingulate cortex, and orbitofrontal cortex. This finding was even reported in individuals with seemingly normal levels of Aβ in both PET and CSF biomarkers (PET-/CSF-) but who later progressed to exhibiting abnormal levels of CSF Aβ (PET-/CSF+). This demonstrates that Aβ fibrils start to accumulate predominantly within certain parts of the DMN in preclinical AD and our data reveals that CSF p-tau231 is a stronger correlate to these early accumulating regions than CSF p-tau217 and CSF p-tau181. Consequently, CSF p-tau231 could be a useful indicator of early Aβ deposition, which can have practical implications for highlighting early AD risk and enrich the enrollment of individuals in the pre-amyloid phase in clinical trials. This was further substantiated by CSF p-tau231 having the largest beta values in relation to Aβ deposition and seemingly becoming abnormal before CSF p-tau217 and CSF p-tau181 when the pathophysiological progression was delineated by Aβ PET Centiloids.

[^{18}F]MK6240 detects paired helical filament (PHF) tau and has shown a high binding affinity for brain homogenate rich in NFTs [58]. CSF p-tau, regardless of phosphorylation site, has been considered as a biomarker of NFT pathology, while other studies propose CSF p-tau as a state marker for brain tau phosphorylation [59], yet the direct association between CSF p-tau and tau PET has been inconsistent. Increases in CSF p-tau occur before both tau PET [20,60,61] and established measures of neuronal death (*e.g.,* neurofilament light, magnetic resonance imaging or [^{18}F]FDG PET), thus CSF p-tau cannot merely reflect NFT leakage from dying neurons. Instead, evidence now documents active secretion of tau in normal and disease conditions [19,62]. In this study, we found that CSF p-tau231 and CSF p-tau217 associated with [^{18}F]MK6240 to the same degree in the whole group and at both CI and CU stages, whereas CSF p-tau181 had weaker associations. In agreement to this, Janelidze et al. previously described that CSF p-tau217 had a consistently greater regional association to tau PET than CSF p-tau181 but CSF p-tau231 was not analyzed in this particular study. Our results are also in line with data suggesting that p-tau217 is a superior clinical biomarker. While no statistical superiority was demonstrated for p-tau217 over p-tau231, we did observe higher fold changes between AD and all other for p-tau217.

On the basis of the evidence presented above, we propose a theoretical framework in which CSF p-tau epitopes become abnormal in a temporally ordered manner as the disease progresses (Fig. 7). Specifically, CSF p-tau231 becomes abnormal first and seems the principal candidate to identify early Aβ seeds in the recently proposed “pre-amyloid phase” [30], which is currently seen as the optimal period for therapeutic intervention. As Aβ accumulates toward Aβ positivity, other p-tau epitopes (p-tau217 and p-tau181) then become abnormal. At the time of tau positivity, CSF p-tau epitopes are almost reaching a plateau. Lately, during neurodegeneration and cognitive abnormalities phases, CSF p-tau epitopes have largely reached a plateau or even demonstrated decrease [63].

We are aware of limitations to this study. Firstly, to definitively describe an ordinal sequence of CSF p-tau biomarkers, from pre-amyloid to symptomatic phases of the disease, longitudinal studies are required. Furthermore, the use of cross-sectional Aβ PET Centiloids as a proxy of time in the disease was

employed and while a gradual Aβ accumulation is observed though AD development, it is not certain that a greater Aβ PET SUVR is indicative of more advanced disease state. Secondly, CSF p-tau biomarkers in this study are compared on two different platforms, with differing detection and capture antibody configurations; N-terminally derived CSF p-tau181 and CSF p-tau217 on the Simoa platform, Mid-terminal CSF p-tau231 by ELISA. Thus, it cannot be ruled out that subtle changes in biomarkers performances are determined by platform differences or antibody superiority. Yet, we believe this is unlikely given that our most promising finding is derived from a traditionally less sensitive technique.

In conclusion, this study documents the pronounced preclinical increases of CSF p-tau biomarkers but specifically highlights CSF p-tau231 which begins to associate with Aβ deposition before the threshold of Aβ PET positivity has occurred and strongly associates with known early Aβ accumulating regions in the DMN. This finding further supports a model of active soluble tau release by cells into the CSF which is related to early Aβ deposition, likely induced by early Aβ seeds. Thus, CSF p-tau231 is a novel candidate for detecting early and emerging Aβ pathology in individuals for the recruitment into therapeutic trials, act as a target engagement biomarker to monitor the effect of Aβ therapeutics or supports the notion of therapeutically targeting tau epitopes in preclinical disease before tau aggregation can be visualized by tau PET.

Table

Table 1. Demographics of the Translational Biomarkers in Aging and Dementia (TRIAD) cohort

	CU Aβ- (*n* = 83)	**CU Aβ+** (*n* = 26)	**CI Aβ-** (*n* = 21)	**CI Aβ+** (*n* = 41)
Females	51 (61)	17 (65)	11 (52)	18 (43)
Age (yr)	55.48 (23.25)	72.20 (7.54)***	67.24 (9.91)***	67.86 (7.88)***
Education (yr)	15.56 (3.15)	14.42 (2.70)	14.94 (4.92)	15.42 (2.98)
***APOE*-e4 carriers**	23 (27)	8 (30)	4 (19)	27 (67)***
MMSE	29.38 (0.90)	29.23 (0.86)	26.76 (2.10)**	23.82 (6.09)***
Aβ PET SUVR	1.23 (0.10)	1.96 (0.42)***	1.25 (0.13)	2.38 (0.42)***
Tau PET SUVR	0.88 (0.10)	1.00 (0.15)	0.85 (0.13)	1.87 (0.61)***
p-tau231 (pg/mL)	8.71 (3.29)	22.14 (17.67)***	9.64 (4.19)	34.32 (19.86)***
p-tau217 (pg/mL)	4.44 (2.88)	15.64 (17.63)***	5.04 (2.30)	26.79 (16.87)***
p-tau181 [Simoa] (pg/mL)	198.83 (122.47)	404.70 (213.81)***	219.96 (91.13)	806.32 (508.79)***
p-tau181 [Lumipulse] (pg/mL)	31.94 (13.95)	58.62 (34.69)***	35.04 (14.03)	95.06 (46.04) ***
Aβ42/40	0.08 (0.01)	0.05 (0.01)***	0.09 (0.01)	0.04 (0.01)***

Data are mean (SD) or n (%); MMSE Mini-Mental State Examination.

**P* values were calculated comparing groups against CU Aβ- subjects using linear regression models for continuous variables and Chi-square tests for categorical variables.

**P*<0.05; ***P*<0.001.

Declarations

ACKNOWLEDGEMENTS

The authors thank all participants of the study and staff at University of Gothenburg, Sahlgrenska University Hospital, McGill University Research Centre for Studies, and Montreal Neurological Institute who supported this project. We thank Cerveau Technologies for MK-6240, and to GE Healthcare for providing the precursor of flutemetamol, and Roche for providing the precursor of RO948. We also thank Kimberley Mauroo for her assistance for the ADx205 epitope mapping.

FUNDING

NJA was supported by the Wallenberg Centre for Molecular and Translational Medicine, Swedish Alzheimer Foundation, the Swedish Dementia Foundation (Demensfonden) and Gamla Tjänarinnor. TAP was supported by the Alzheimer Society Research Program and the Canadian Consortium on Neurodegeneration in Aging. TKK is supported by the BrightFocus Foundation (#A2020812F), the Swedish Alzheimer Foundation (Alzheimerfonden; #AF-930627), the Swedish Brain Foundation (Hjärnfonden; #FO2020-0240), the Swedish Parkinson Foundation (Parkinsonfonden; #1252/20), the Swedish Dementia Foundation (Demensförbundet), Gamla Tjänarinnor Foundation, the Aina (Ann) Wallströms and Mary-Ann Sjöbloms Foundation, the Agneta Prytz-Folkes & Gösta Folkes Foundation (#2020-00124), the Gun and Bertil Stohnes Foundation, and the Anna Lisa and Brother Björnsson's Foundation. HZ is a Wallenberg Scholar supported by grants from the Swedish Research Council (#2018-02532), the European Research Council (#681712), Swedish State Support for Clinical Research (#ALFGBG-720931), the Alzheimer Drug Discovery Foundation (ADDF), USA (#201809-2016862), the European Union's Horizon 2020 research and innovation programme under the Marie Skłodowska-Curie grant agreement No 860197 (MIRIADE), and the UK Dementia Research Institute at UCL. KB was supported by the Alzheimer Drug Discovery Foundation (ADDF; #RDAPB-201809-2016615), the Swedish Research Council (#2017-00915), the Swedish Alzheimer Foundation (#AF-742881), Hjärnfonden, Sweden (#FO2017-0243), and a grant (#ALFGBG-715986) from the Swedish state under the agreement between the Swedish government and the County Councils, the ALF-agreement. TRIAD is supported by the Canadian Institutes of Health Research (CIHR) [MOP-11-51-31; RFN 152985**,** 159815, 162303], Canadian Consortium of Neurodegeneration and Aging (CCNA; MOP-11-51-31 -team 1), Weston Brain Institute, Brain Canada Foundation (CFI Project 34874; 33397), the Fonds de Recherche du Québec – Santé (FRQS; Chercheur Boursier, 2020-VICO-279314). TAP, P.R-N and SG are members of the CIHR-CCNA Canadian Consortium of Neurodegeneration in Aging.

AUTHOR CONTRIBUTIONS

NJA, ALB, TAP, TKK, HK, OH, KB and PR-N conceived the study. Data acquisition was achieved NJA, TKK, JLR. NJA and ALB performed statistical analysis. ALB, TAP, SJ, JT, MS, MC PR-N designed and implemented MRI and PET acquisition protocols, as well as performed image processing and quality control. SG, HZ, OH, KB and PR-N recruited participants, and collected clinical data. NJA, ALB, TAP, TKK, ERZ, SG, HZ, KB and PR-N interpreted the data. NJA, ALB, ERZ, KB and PR-N drafted the initial manuscript. All authors contributed to revision and editing of the manuscript

COMPETING INTERESTS

HZ has served at scientific advisory boards for Denali, Roche Diagnostics, Wave, Samumed, Siemens Healthineers, Pinteon Therapeutics and CogRx, and has given lectures in symposia sponsored by Fujirebio, Alzecure and Biogen. KB has served as a consultant, at advisory boards, or at data monitoring committees for Abcam, Axon, Biogen, JOMDD/Shimadzu. Julius Clinical, Lilly, MagQu, Novartis, Roche Diagnostics, and Siemens Healthineers, and is a co-founder of Brain Biomarker Solutions in Gothenburg AB (BBS), which is a part of the GU Ventures Incubator Program. CF, and ES and are employee of ADx NeuroSciences, Gent, Belgium, EVM is a co-founder of ADx NeuroSciences. The other authors declare no competing interest.

References

1 Scheltens, P. *et al.* Alzheimer's disease. *Lancet* **388**, 505-517, doi:10.1016/S0140-6736(15)01124-1 (2016).

2 Olsson, B. *et al.* CSF and blood biomarkers for the diagnosis of Alzheimer's disease: a systematic review and meta-analysis. *Lancet Neurol* **15**, 673-684, doi:10.1016/S1474-4422(16)00070-3 (2016).

3 Hansson, O. *et al.* Association between CSF biomarkers and incipient Alzheimer's disease in patients with mild cognitive impairment: a follow-up study. *Lancet Neurol* **5**, 228-234, doi:10.1016/S1474-4422(06)70355-6 (2006).

4 Shaw, L. M. *et al.* Cerebrospinal fluid biomarker signature in Alzheimer's disease neuroimaging initiative subjects. *Ann Neurol* **65**, 403-413, doi:10.1002/ana.21610 (2009).

5 Vos, S. J. *et al.* Preclinical Alzheimer's disease and its outcome: a longitudinal cohort study. *Lancet Neurol* **12**, 957-965, doi:10.1016/S1474-4422(13)70194-7 (2013).

6 Schindler, S. E. *et al.* Emerging cerebrospinal fluid biomarkers in autosomal dominant Alzheimer's disease. *Alzheimers Dement* **15**, 655-665, doi:10.1016/j.jalz.2018.12.019 (2019).

7 Jack, C. R., Jr. *et al.* NIA-AA Research Framework: Toward a biological definition of Alzheimer's disease. *Alzheimers Dement* **14**, 535-562, doi:10.1016/j.jalz.2018.02.018 (2018).

8 Riemenschneider, M. *et al.* Phospho-tau/total tau ratio in cerebrospinal fluid discriminates Creutzfeldt-Jakob disease from other dementias. *Mol Psychiatry* **8**, 343-347, doi:10.1038/sj.mp.4001220 (2003).

9 Skillback, T. *et al.* Diagnostic performance of cerebrospinal fluid total tau and phosphorylated tau in Creutzfeldt-Jakob disease: results from the Swedish Mortality Registry. *JAMA Neurol* **71**, 476-483, doi:10.1001/jamaneurol.2013.6455 (2014).

10 Schoonenboom, N. S. *et al.* Cerebrospinal fluid markers for differential dementia diagnosis in a large memory clinic cohort. *Neurology* **78**, 47-54, doi:10.1212/WNL.0b013e31823ed0f0 (2012).

11 Hampel, H. *et al.* Measurement of phosphorylated tau epitopes in the differential diagnosis of Alzheimer disease: a comparative cerebrospinal fluid study. *Arch Gen Psychiatry* **61**, 95-102, doi:10.1001/archpsyc.61.1.95 (2004).

12 Leuzy, A. *et al.* Diagnostic Performance of RO948 F 18 Tau Positron Emission Tomography in the Differentiation of Alzheimer Disease From Other Neurodegenerative Disorders. *JAMA Neurol*, doi:10.1001/jamaneurol.2020.0989 (2020).

13 La Joie, R. *et al.* Associations between [(18)F]AV1451 tau PET and CSF measures of tau pathology in a clinical sample. *Neurology* **90**, e282-e290, doi:10.1212/WNL.0000000000004860 (2018).

14 Maia, L. F. *et al.* Changes in amyloid-beta and Tau in the cerebrospinal fluid of transgenic mice overexpressing amyloid precursor protein. *Sci Transl Med* **5**, 194re192, doi:10.1126/scitranslmed.3006446 (2013).

15 Schelle, J. *et al.* Prevention of tau increase in cerebrospinal fluid of APP transgenic mice suggests downstream effect of BACE1 inhibition. *Alzheimers Dement* **13**, 701-709, doi:10.1016/j.jalz.2016.09.005 (2017).

16 De Felice, F. G. *et al.* Alzheimer's disease-type neuronal tau hyperphosphorylation induced by A beta oligomers. *Neurobiol Aging* **29**, 1334-1347, doi:10.1016/j.neurobiolaging.2007.02.029 (2008).

17 Sackmann, C. & Hallbeck, M. Oligomeric amyloid-beta induces early and widespread changes to the proteome in human iPSC-derived neurons. *Sci Rep* **10**, 6538, doi:10.1038/s41598-020-63398-6 (2020).

18 Barthelemy, N. R. *et al.* A soluble phosphorylated tau signature links tau, amyloid and the evolution of stages of dominantly inherited Alzheimer's disease. *Nat Med* **26**, 398-407, doi:10.1038/s41591-020-0781-z (2020).

19 Sato, C. *et al.* Tau Kinetics in Neurons and the Human Central Nervous System. *Neuron* **97**, 1284-1298 e1287, doi:10.1016/j.neuron.2018.02.015 (2018).

20 Bateman, R. J. *et al.* Clinical and biomarker changes in dominantly inherited Alzheimer's disease. *N Engl J Med* **367**, 795-804, doi:10.1056/NEJMoa1202753 (2012).

21 Toledo, J. B., Xie, S. X., Trojanowski, J. Q. & Shaw, L. M. Longitudinal change in CSF Tau and Abeta biomarkers for up to 48 months in ADNI. *Acta Neuropathol* **126**, 659-670, doi:10.1007/s00401-013-1151-4 (2013).

22 Brunello, C. A., Merezhko, M., Uronen, R. L. & Huttunen, H. J. Mechanisms of secretion and spreading of pathological tau protein. *Cell Mol Life Sci* **77**, 1721-1744, doi:10.1007/s00018-019-03349-1 (2020).

23 Ishiguro, K. *et al.* Phosphorylated tau in human cerebrospinal fluid is a diagnostic marker for Alzheimer's disease. *Neurosci Lett* **270**, 91-94, doi:10.1016/s0304-3940(99)00476-0 (1999).

24 Janelidze, S. *et al.* Cerebrospinal fluid p-tau217 performs better than p-tau181 as a biomarker of Alzheimer's disease. *Nat Commun* **11**, 1683, doi:10.1038/s41467-020-15436-0 (2020).

25 Russell, C. L. *et al.* Comprehensive Quantitative Profiling of Tau and Phosphorylated Tau Peptides in Cerebrospinal Fluid by Mass Spectrometry Provides New Biomarker Candidates. *J Alzheimers Dis* **55**, 303-313, doi:10.3233/JAD-160633 (2017).

26 Buerger, K. *et al.* Differential diagnosis of Alzheimer disease with cerebrospinal fluid levels of tau protein phosphorylated at threonine 231. *Arch Neurol* **59**, 1267-1272, doi:10.1001/archneur.59.8.1267 (2002).

27 Barthelemy, N. R. *et al.* Cerebrospinal fluid phospho-tau T217 outperforms T181 as a biomarker for the differential diagnosis of Alzheimer's disease and PET amyloid-positive patient identification. *Alzheimers Res Ther* **12**, 26, doi:10.1186/s13195-020-00596-4 (2020).

28 Karikari, T. K. *et al.* Head-to-head comparison of clinical performance of CSF phospho-tau T181 and T217 biomarkers for Alzheimer's disease diagnosis. *Alzheimers Dement*, doi:10.1002/alz.12236 (2020).

29 Suarez-Calvet, M. *et al.* Novel tau biomarkers phosphorylated at T181, T217 or T231 rise in the initial stages of the preclinical Alzheimer's continuum when only subtle changes in Abeta pathology are detected. *EMBO Mol Med*, e12921, doi:10.15252/emmm.202012921 (2020).

30 Uhlmann, R. E. *et al.* Acute targeting of pre-amyloid seeds in transgenic mice reduces Alzheimer-like pathology later in life. *Nat Neurosci* **23**, 1580-1588, doi:10.1038/s41593-020-00737-w (2020).

31 Horowitz, P. M. *et al.* Early N-terminal changes and caspase-6 cleavage of tau in Alzheimer's disease. *J Neurosci* **24**, 7895-7902, doi:10.1523/JNEUROSCI.1988-04.2004 (2004).

32 De Vos, A. A novel conformational, phospho-Threonine 231 specific assay for CSF protein tau. *J Prev Alzheimers Dis* (2016).

33 Cselenyi, Z. *et al.* Clinical validation of 18F-AZD4694, an amyloid-beta-specific PET radioligand. *J Nucl Med* **53**, 415-424, doi:10.2967/jnumed.111.094029 (2012).

34 Pascoal, T. A. *et al.* In vivo quantification of neurofibrillary tangles with [(18)F]MK-6240. *Alzheimers Res Ther* **10**, 74, doi:10.1186/s13195-018-0402-y (2018).

35 Therriault, J. *et al.* Association of Apolipoprotein E epsilon4 With Medial Temporal Tau Independent of Amyloid-beta. *JAMA Neurol* **77**, 470-479, doi:10.1001/jamaneurol.2019.4421 (2020).

36 Pascoal, T. A. *et al.* 18F-MK-6240 PET for early and late detection of neurofibrillary tangles. *Brain* **143**, 2818-2830, doi:10.1093/brain/awaa180 (2020).

37 Pascoal, T. A. *et al.* Amyloid and tau signatures of brain metabolic decline in preclinical Alzheimer's disease. *Eur J Nucl Med Mol Imaging* **45**, 1021-1030, doi:10.1007/s00259-018-3933-3 (2018).

38 Therriault, J. *et al.* Determining Amyloid-beta positivity using [(18)F]AZD4694 PET imaging. *J Nucl Med*, doi:10.2967/jnumed.120.245209 (2020).

39 Klunk, W. E. *et al.* The Centiloid Project: standardizing quantitative amyloid plaque estimation by PET. *Alzheimers Dement* **11**, 1-15 e11-14, doi:10.1016/j.jalz.2014.07.003 (2015).

40 Rowe, C. C. *et al.* Standardized Expression of 18F-NAV4694 and 11C-PiB beta-Amyloid PET Results with the Centiloid Scale. *J Nucl Med* **57**, 1233-1237, doi:10.2967/jnumed.115.171595 (2016).

41 Braak, H. & Braak, E. Neuropathological stageing of Alzheimer-related changes. *Acta Neuropathol* **82**, 239-259, doi:10.1007/BF00308809 (1991).

42 Braak, H., Alafuzoff, I., Arzberger, T., Kretzschmar, H. & Del Tredici, K. Staging of Alzheimer disease-associated neurofibrillary pathology using paraffin sections and immunocytochemistry. *Acta Neuropathol* **112**, 389-404, doi:10.1007/s00401-006-0127-z (2006).

43 Mathotaarachchi, S. *et al.* VoxelStats: A MATLAB Package for Multi-Modal Voxel-Wise Brain Image Analysis. *Front Neuroinform* **10**, 20, doi:10.3389/fninf.2016.00020 (2016).

44 Worsley, K. J., Taylor, J. E., Tomaiuolo, F. & Lerch, J. Unified univariate and multivariate random field theory. *Neuroimage* **23 Suppl 1**, S189-195, doi:10.1016/j.neuroimage.2004.07.026 (2004).

45 Wu, J. W. *et al.* Small misfolded Tau species are internalized via bulk endocytosis and anterogradely and retrogradely transported in neurons. *J Biol Chem* **288**, 1856-1870, doi:10.1074/jbc.M112.394528 (2013).

46 Mirbaha, H., Holmes, B. B., Sanders, D. W., Bieschke, J. & Diamond, M. I. Tau Trimers Are the Minimal Propagation Unit Spontaneously Internalized to Seed Intracellular Aggregation. *J Biol Chem* **290**, 14893-14903, doi:10.1074/jbc.M115.652693 (2015).

47 Santos, J. R. F. *et al.* Validation of a prototype tau Thr231 phosphorylation CSF ELISA as a potential biomarker for Alzheimer's disease. *J Neural Transm (Vienna)* **126**, 339-348, doi:10.1007/s00702-019-01982-5 (2019).

48 Spiegel, J. *et al.* Greater specificity for cerebrospinal fluid P-tau231 over P-tau181 in the differentiation of healthy controls from Alzheimer's disease. *J Alzheimers Dis* **49**, 93-100, doi:10.3233/JAD-150167 (2016).

49 Blennow, K., Vanmechelen, E. & Hampel, H. CSF total tau, Abeta42 and phosphorylated tau protein as biomarkers for Alzheimer's disease. *Mol Neurobiol* **24**, 87-97, doi:10.1385/MN:24:1-3:087 (2001).

50 Glodzik-Sobanska, L. *et al.* The effects of normal aging and ApoE genotype on the levels of CSF biomarkers for Alzheimer's disease. *Neurobiol Aging* **30**, 672-681, doi:10.1016/j.neurobiolaging.2007.08.019 (2009).

51 Kidemet-Piskac, S. *et al.* Evaluation of cerebrospinal fluid phosphorylated tau231 as a biomarker in the differential diagnosis of Alzheimer's disease and vascular dementia. *CNS Neurosci Ther* **24**, 734-740, doi:10.1111/cns.12814 (2018).

52 Mitchell, A. J. CSF phosphorylated tau in the diagnosis and prognosis of mild cognitive impairment and Alzheimer's disease: a meta-analysis of 51 studies. *J Neurol Neurosurg Psychiatry* **80**, 966-975, doi:10.1136/jnnp.2008.167791 (2009).

53 Augustinack, J. C., Schneider, A., Mandelkow, E. M. & Hyman, B. T. Specific tau phosphorylation sites correlate with severity of neuronal cytopathology in Alzheimer's disease. *Acta Neuropathol* **103**, 26-35, doi:10.1007/s004010100423 (2002).

54 Ercan-Herbst, E. *et al.* A post-translational modification signature defines changes in soluble tau correlating with oligomerization in early stage Alzheimer's disease brain. *Acta Neuropathol Commun* **7**, 192, doi:10.1186/s40478-019-0823-2 (2019).

55 Castellani, R. J. & Perry, G. Tau Biology, Tauopathy, Traumatic Brain Injury, and Diagnostic Challenges. *J Alzheimers Dis* **67**, 447-467, doi:10.3233/JAD-180721 (2019).

56 Amniai, L. *et al.* Alzheimer disease specific phosphoepitopes of Tau interfere with assembly of tubulin but not binding to microtubules. *FASEB J* **23**, 1146-1152, doi:10.1096/fj.08-121590 (2009).

57 Palmqvist, S. *et al.* Earliest accumulation of beta-amyloid occurs within the default-mode network and concurrently affects brain connectivity. *Nat Commun* **8**, 1214, doi:10.1038/s41467-017-01150-x (2017).

58 Malarte, M. L., Nordberg, A. & Lemoine, L. Characterization of MK6240, a tau PET tracer, in autopsy brain tissue from Alzheimer's disease cases. *Eur J Nucl Med Mol Imaging*, doi:10.1007/s00259-020-05035-y (2020).

59 Blennow, K. & Hampel, H. CSF markers for incipient Alzheimer's disease. *Lancet Neurol* **2**, 605-613, doi:10.1016/s1474-4422(03)00530-1 (2003).

60 Mattsson-Carlgren, N. *et al.* Abeta deposition is associated with increases in soluble and phosphorylated tau that precede a positive Tau PET in Alzheimer's disease. *Sci Adv* **6**, eaaz2387, doi:10.1126/sciadv.aaz2387 (2020).

61 Gordon, B. A. *et al.* Tau PET in autosomal dominant Alzheimer's disease: relationship with cognition, dementia and other biomarkers. *Brain* **142**, 1063-1076, doi:10.1093/brain/awz019 (2019).

62 Pooler, A. M., Phillips, E. C., Lau, D. H., Noble, W. & Hanger, D. P. Physiological release of endogenous tau is stimulated by neuronal activity. *EMBO Rep* **14**, 389-394, doi:10.1038/embor.2013.15 (2013).

63 Sutphen, C. L. *et al.* Longitudinal decreases in multiple cerebrospinal fluid biomarkers of neuronal injury in symptomatic late onset Alzheimer's disease. *Alzheimers Dement* **14**, 869-879, doi:10.1016/j.jalz.2018.01.012 (2018).

Figures

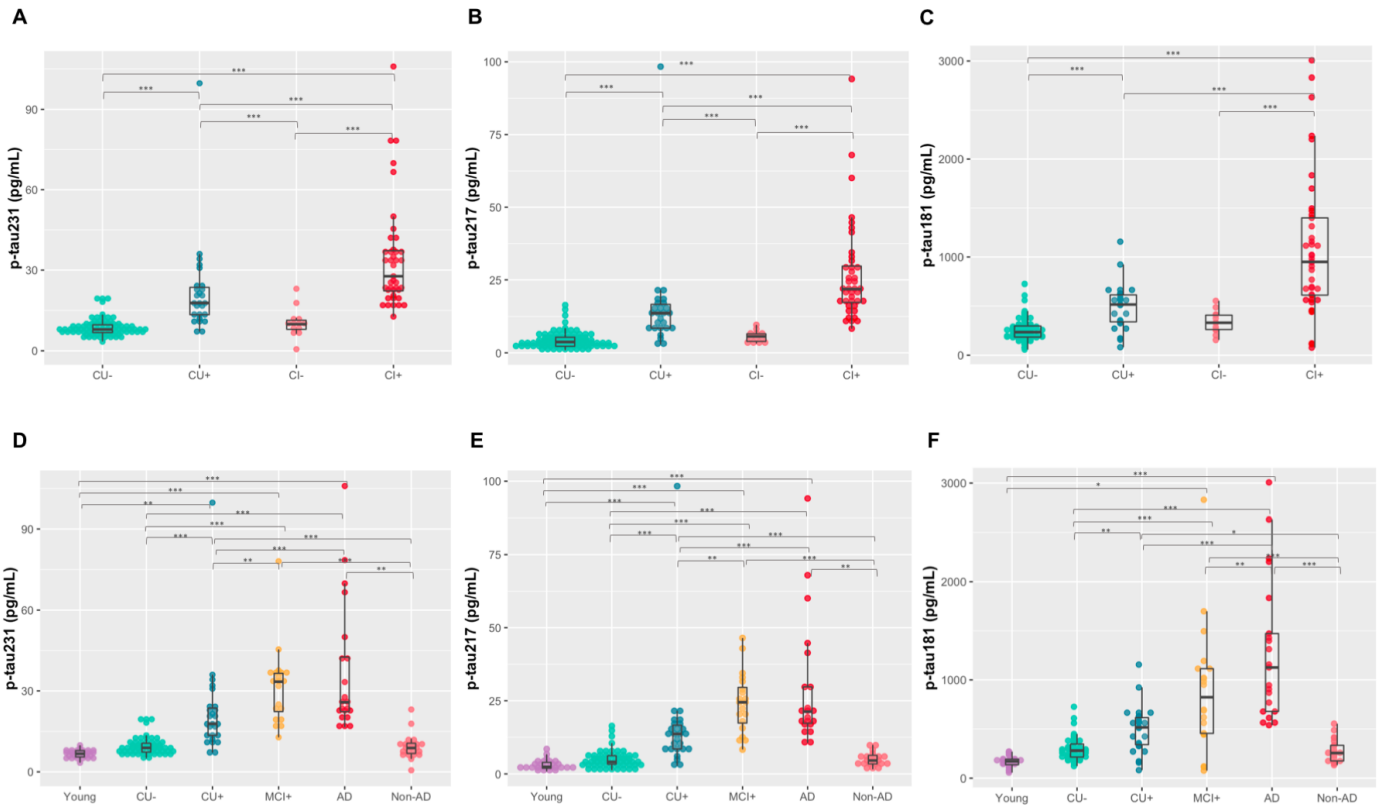

Figure 1

Phosphorylated tau CSF epitopes by group. Distribution of CSF biomarkers concentrations across groups showing higher biomarker levels associated with Aβ positivity. CU-: cognitively unimpaired Aβ negative; CU+: cognitively unimpaired Aβ positive; CI-: cognitively impaired Aβ negative; CI+: cognitively impaired Aβ positive; MCI+: mild cognitively impaired Aβ positive; AD: Alzheimer's disease dementia; Non-AD: mild

cognitively impaired Aβ negative and frontotemporal dementia (FTD). ***P<0.001; **P<0.01; *P<0.05 (Tukey HSD adjusted).

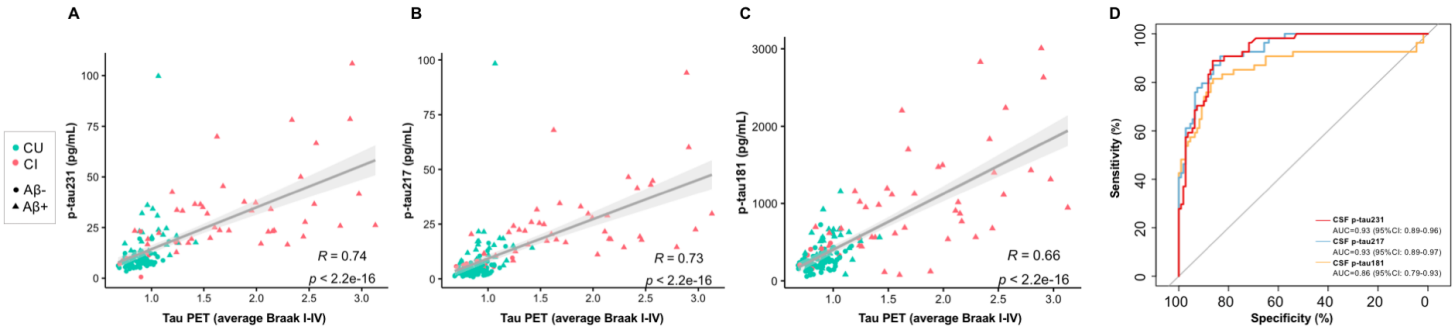

Figure 2

The topography of phosphorylated tau CSF epitopes associations with tau PET. T-parametric maps show the voxel-wise association between CSF biomarkers and [18F]MK6240 in all participants (A) as well as within cognitively impaired (CI; B) and unimpaired groups (CU; C). Models were adjusted for age and sex and RFT was used to account for multiple comparisons (significant t-values > 3.1).

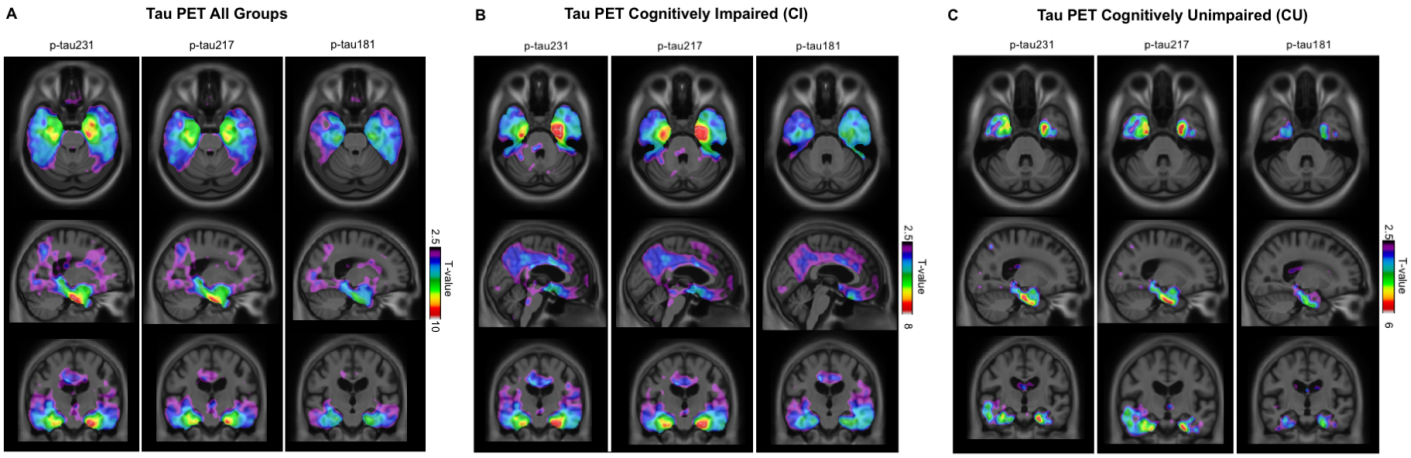

Figure 3

Phosphorylated tau CSF epitopes and Aβ PET associations. Spearman rank correlations between CSF biomarkers and Aβ PET ([18F]AZD4694) across all groups show p-tau231 as having the highest correlation coefficient (A-C). The accuracy of CSF biomarkers in distinguishing Aβ PET status (positive vs negative) is evidenced by AUCs as shown in (D). CU: cognitively unimpaired; CI: cognitively impaired.

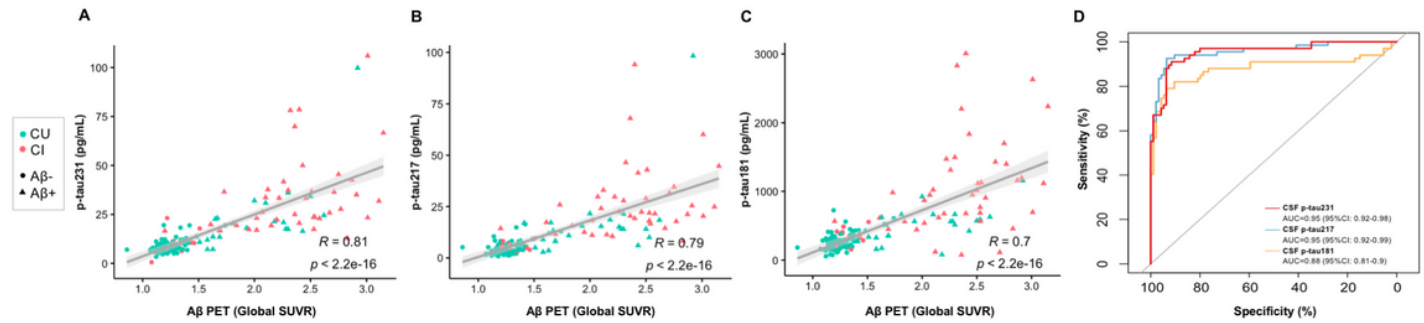

Figure 4

The topography of phosphorylated tau CSF epitopes with Aβ PET. T-parametric maps show the voxel-wise association between CSF biomarkers and [18F]AZD4694 in all participants (A) as well as within cognitively impaired (CI; B) and unimpaired groups (CU; C). Models were adjusted by age and sex and RFT was used to account for multiple comparisons (significant t-values > 3.1).

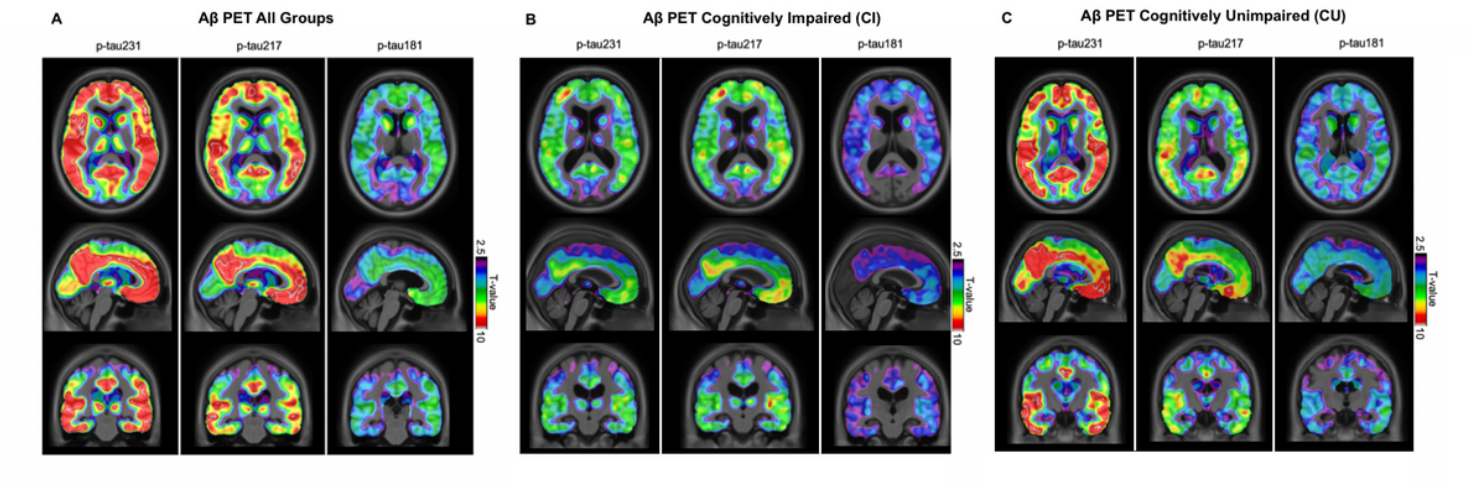

Figure 5

Phosphorylated tau CSF epitopes effect size on Aβ PET in the CU group. The dot plot shows the average slope (beta) values by ROI for each of the CSF biomarkers. The beta value was derived from linear models that had Aβ PET as the outcome measure, the CSF biomarkers were the predictors and the covariates were sex and age. These models were performed at the voxel level and the CSF p-tau beta values of each voxel were averaged within ROIs. Were included in the ROIs only the voxels that had a significant association between Aβ PET and all of the CSF biomarkers evaluated here. In addition, CSF p-tau biomarkers were plotted (B) as a function of Aβ PET deposition (in Centiloids), which was used to infer AD pathology progression. Dashed line indicates the biomarker cut off for positivity.

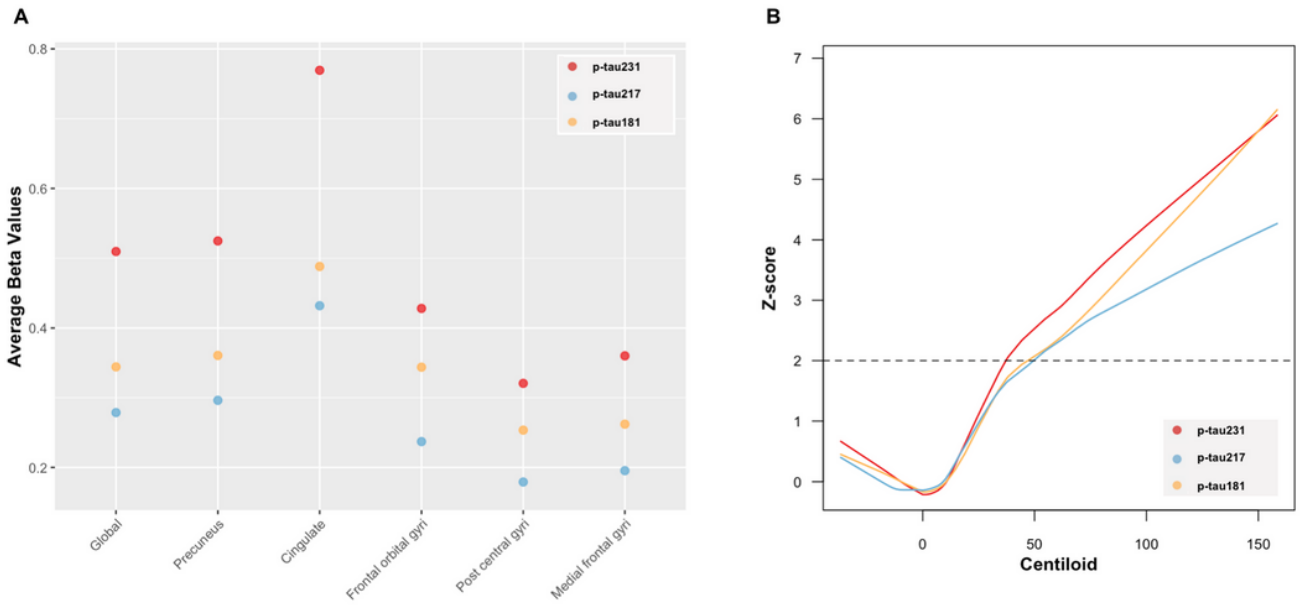

Figure 6

P-tau231 as an early biomarker of Aβ pathology. T-parametric maps (A) show the voxel-wise association between CSF biomarkers (p-tau231, p-tau217 and p-tau181) and [18F]AZD4694 in Aβ-negative cognitively unimpaired (CU; A) subjects. Models were adjusted for age and sex and RFT was used to account for multiple comparisons (significant t-values > 3.1). In addition, CSF p-tau biomarkers were plotted (B) as a function of Aβ PET deposition (in Centiloids) in the CU group, which was used to infer AD pathology progression. Dashed line indicates the biomarker cut off for positivity.

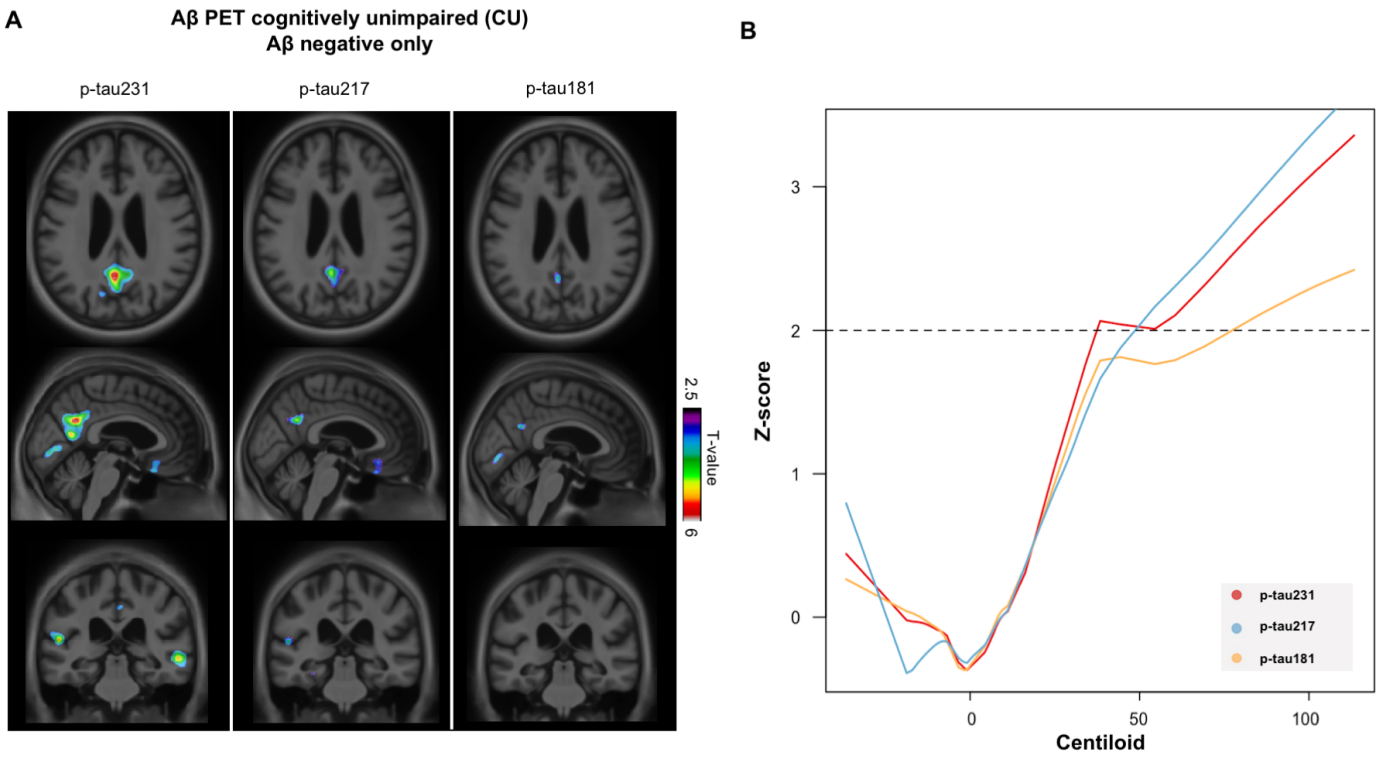

Figure 7

The theoretical framework proposed presents a temporarily ordered progression of CSF p-tau epitopes in the context of the AD continuum, in which we hypothesize CSF p-tau231 as the first biomarker to become altered in the pre-amyloid phase, being then followed by p-tau217 and p-tau181 at pre-clinical and clinical stages.

Supplementary Files

This is a list of supplementary files associated with this preprint. Click to download.

- SupplementNatureCommsV2.docx